

Random matrix model approach to chiral symmetry

J.J.M. Verbaarschot^a

^aDept. of Physics, SUNY at Stony Brook, Stony Brook, NY 11794

We review the application of random matrix theory (RMT) to chiral symmetry in QCD. Starting from the general philosophy of RMT we introduce a chiral random matrix model with the global symmetries of QCD. Exact results are obtained for universal properties of the Dirac spectrum: i) finite volume corrections to valence quark mass dependence of the chiral condensate, and ii) microscopic fluctuations of Dirac spectra. Comparisons with lattice QCD simulations are made. Most notably, the variance of the number of levels in an interval containing n levels on average is suppressed by a factor $(\log n)/\pi^2 n$. An extension of the random matrix model to nonzero temperatures and chemical potential provides us with a schematic model of the chiral phase transition. In particular, this elucidates the nature of the quenched approximation at nonzero chemical potential.

1. INTRODUCTION

Random matrix theories have been applied to many areas of physics ranging from nuclear physics [1] to quantum gravity [2] and neural networks [3]. In general, one can divide RMT applications into two different groups. First, as a description of universal fluctuations of an observable expressed in terms of its average value. For example, the Hauser-Feshbach formula [4,5] and universal conductance fluctuations [6]. Second, RMT can be used as a schematic model for problems involving disorder. Well-known examples in this category are the Anderson Model [7], the Gross-Witten model [8] and models for neural networks [3].

In this lecture we will review the application of RMT to chiral symmetry in QCD. Before discussing both types of applications, we introduce the concept of universality within this context.

As has been argued, in particular by Leutwyler and Smilga [9], the mass dependence of the QCD partition function in the 'mesoscopic' range

$$\frac{1}{\Lambda} \ll V^{1/4} \ll \frac{1}{\sqrt{mV}}, \quad (1)$$

where m is the quark mass, and Λ is a typical hadronic scale, is given by

$$Z_{\text{eff}}(M, \theta) = \int_{U \in SU(N_f)} dU e^{\text{Re} V \Sigma \text{Tr} M U e^{i\theta/N_f}}. \quad (2)$$

Here, M is the mass matrix, θ is the vacuum an-

gle, and $\Sigma = |\langle \bar{q}q \rangle|$. However, QCD is not the only theory that can be mapped onto this effective partition function. In section 3, we will introduce a random matrix model that can be reduced to (2) as well. This allows us to formulate universality: different theories with the same low-energy effective partition function have common properties.

2. DIRAC SPECTRUM

Our main focus will be on the spectrum of the Dirac operator,

$$i\gamma D\phi_k = \lambda_k \phi_k, \quad (3)$$

with spectral density $\rho(\lambda) = \sum \delta(\lambda - \lambda_k)$. The density of small eigenvalues is related to the chiral condensate by means of the Banks-Casher formula [10]

$$|\langle \bar{\psi}\psi \rangle| = \frac{\pi\rho(0)}{V}, \quad (4)$$

where it is understood that the thermodynamic limit is taken before the chiral limit. Since $\{\gamma_5, i\gamma D\} = 0$, the nonzero eigenvalues occur in pairs $\pm\lambda_k$. The smallest eigenvalue is of order $\lambda_{\min} \approx \pi/\Sigma V$. In the QCD partition function, the Dirac eigenvalues and the quark mass occur only in the combination $m^2 + \lambda_k^2$. Therefore, it is natural to expect that universal features of the Dirac spectrum can only be found in a region con-

sistent with (1) which, in terms of the eigenvalues, can be expressed as $|\lambda_k| \ll \sqrt{\lambda_{\min}\Lambda} \ll \Lambda$.

In order to identify a universal quantity, let us consider the mass dependence of the QCD partition function in the range (1),

$$\frac{\langle \prod_{k,f} (\lambda_k^2 + m_f^2) \rangle}{\langle \prod_{k,f} \lambda_k^2 \rangle} = Z_{\text{eff}}(M, \theta). \quad (5)$$

Here, the average $\langle \dots \rangle$ is over gauge field configurations weighted by the QCD action. By expanding both sides in powers of m_f we find an infinite family of sum-rules [9]. The simplest sum rule,

$$\frac{1}{V^2} \sum_{\lambda_k > 0} \frac{1}{\lambda_k^2} = \frac{\Sigma^2}{4N_f}, \quad (6)$$

has been verified for the instanton liquid model of the QCD vacuum [11]. If we write the sum in (6) as an integral over the spectral density and introduce the microscopic variable $u = \lambda V \Sigma$, we find

$$\int_0^\infty \frac{1}{V \Sigma} \rho\left(\frac{u}{V \Sigma}\right) \frac{du}{u^2} = \frac{1}{4N_f}. \quad (7)$$

What enters in (7) is the microscopic spectral density, which in the range $\lambda \ll \sqrt{\lambda_{\min}\Lambda}$ can be approximated by its thermodynamic limit

$$\rho_S(u) = \lim_{V \rightarrow \infty} \frac{1}{V \Sigma} \rho\left(\frac{u}{V \Sigma}\right). \quad (8)$$

The existence of this limit follows from the spacing of the eigenvalues near zero virtuality as $\Delta\lambda \sim 1/V$ in the broken phase.

Our conjecture is that $\rho_S(u)$ is a universal function that can be obtained from a random matrix model with the global symmetries of QCD. Note that $\rho_S(u)$ is not fixed by $Z_{\text{eff}}(M, \theta)$. Before defining this model we discuss the well-known application of RMT to spectra of complex systems.

3. SPECTRAL CORRELATIONS OF COMPLEX SYSTEMS

RMT has a long history of successes in explaining the statistical properties of nuclear spectra [1]. More recently, spectral correlations have been investigated in the context of quantum chaos [12]. The starting point is the observation that the

scale of variations of the average spectral density and the fluctuations of the spectral density separate. This allows us to unfold the spectrum. From the original spectrum $\{\lambda_k\}$ we construct an unfolded spectrum $\{\lambda'_k\}$ with average spectral density equal to 1. This is achieved by $\int^{\lambda'_k} \bar{\rho}(\lambda) d\lambda = \lambda_k$, where $\bar{\rho}(\lambda)$ is the average spectral density.

A variety of statistics has been introduced to analyze the spectral correlations of the *unfolded* spectrum. The best known statistic is the nearest neighbor spacing distribution $P(S)$. A theoretically simpler statistic is the distribution of the number of levels, $n_k(n)$, in an interval of length n . In this lecture, we will consider its variance denoted by $\Sigma_2(n)$, and the $\Delta_3(n)$ statistic [13] obtained by a smoothening of $\Sigma_2(n)$.

The above statistics can be obtained analytically for the invariant random matrix ensembles. They are ensembles of Hermitean matrices with probability distribution given by $P(H) \sim \exp -\text{Tr} H^\dagger H$. Three different invariant random matrix ensembles can be constructed: the Gaussian Orthogonal Ensemble (GOE) when H is real, the Gaussian Unitary Ensemble (GUE) when H is complex and the Gaussian Symplectic Ensemble (GSE) when H is quaternion real. They are characterized by the Dyson index β , which is equal to 1, 2 and 4, respectively. The relevant random matrix ensemble is determined by the anti-unitary symmetry of the Hamiltonian H . If there is no anti-unitary symmetry the spectral correlations are given by the GUE. If the anti-unitary symmetry operator A satisfies $A^2 = 1$, it is possible to find a basis in which H is real, if $A^2 = -1$, one can construct a basis in which H becomes quaternion real [1]. Spectral correlations are given by the GOE and the GSE, respectively.

For simplicity we only give approximate results for the above statistics. The nearest neighbor spacing distribution is well approximated by the Wigner surmise given by $P(S) \sim S^\beta \exp(-a_\beta S^2)$, where a_β is a constant. For $n \geq 1$ the number variance is given by $\Sigma_2(n) \sim (2/\pi^2\beta) \log n$ and the Δ_3 -statistic $\Delta_3(n) \sim \Sigma_2(n)/2$. The RMT results for these statistics should be contrasted with the results for uncorrelated eigenvalues. Then,

$P(S) = S$, $\Sigma_2(n) = n$ and $\Delta_3(n) = n/15$. In particular, we wish to emphasize that long range spectral correlations are strongly suppressed with respect to uncorrelated eigenvalues.

Spectral statistics of a large variety of systems have been compared to RMT. We wish to mention, the nuclear data ensemble [1], the zeros of Riemann's ζ -function [14], the correlations of resonances in electromagnetic resonance cavities [15], and the spectrum of the Sinai billiard [16]. The main conclusion is that if the corresponding classical system is chaotic, the microscopic correlations of the spectrum within an irreducible subspace are given by the RMT with the corresponding anti-unitary symmetry.

4. CHIRAL RANDOM MATRIX MODEL

In this section we will introduce a random matrix model for the QCD partition function. Our hope is to construct a model that reproduces both the microscopic spectral density and the correlations in the bulk of the spectrum. In the spirit of the invariant RMT we construct a model for the Dirac operator with the global symmetries of the QCD partition function as input, but otherwise gaussian random matrix elements. The chiral random matrix model (chRMM) that obeys these conditions is defined by [11,17,18]

$$Z_\nu^\beta = \int DW \prod_{f=1}^{N_f} \det(\mathcal{D} + m_f) e^{-\frac{N\Sigma^2\beta}{4} \text{Tr} W^\dagger W}, \quad (9)$$

where

$$\mathcal{D} = \begin{pmatrix} 0 & iW \\ iW^\dagger & 0 \end{pmatrix}, \quad (10)$$

and W is a rectangular $n \times m$ matrix with $\nu = |n - m|$ and $N = n + m$. The matrix elements of W are either real ($\beta = 1$, chiral Gaussian Orthogonal Ensemble (chGOE)), complex ($\beta = 2$, chiral Gaussian Unitary Ensemble (chGUE)), or quaternion real ($\beta = 4$, chiral Gaussian Symplectic Ensemble (chGSE)). A precursor of this model was introduced within the framework of the instanton liquid partition function [19]. This model reproduces the following symmetries of the QCD partition function: *i*) The $U_A(1)$ symmetry. All

nonzero eigenvalues of the random matrix Dirac operator occur in pairs $\pm\lambda$. *ii*) The topological structure of the QCD partition function. The matrix \mathcal{D} has exactly $|\nu| \equiv |n - m|$ zero eigenvalues. This identifies ν as the topological sector of the model. *iii*) The flavor symmetry is the same as in QCD. For $\beta = 2$, it is $SU(N_f) \times SU(N_f)$. For $\beta = 1$, it is $SU(2N_f)$, and for $\beta = 4$, it is $SU(N_f)$. *iv*) The chiral symmetry is broken spontaneously for two or more flavors according to the pattern [20] $SU(N_f) \times SU(N_f)/SU(N_f)$, $SU(2N_f)/Sp(N_f)$ and $SU(N_f)/O(N_f)$ for $\beta = 2, 1$ and 4 , respectively, the same as in QCD [21]. The chiral condensate in this model follows from the Banks-Casher relation, $\Sigma = \lim_{N \rightarrow \infty} \pi\rho(0)/N$. (N is interpreted as the (dimensionless) volume of space time.) *v*) The anti-unitary symmetries. For three and more colors with fundamental fermions the Dirac operator has no anti-unitary symmetries, and we choose $\beta = 2$ in (9). For $N_c = 2$ and fundamental fermions the Dirac operator satisfies $[C\tau_2 K, i\gamma D] = 0$, where C is the charge conjugation matrix and K is the complex conjugation operator. Because, $(C\tau_2 K)^2 = 1$, the matrix elements of the Dirac operator can always be chosen real, and the corresponding random matrix ensemble is the chGOE. For two or more colors with fermions in the adjoint representation $i\gamma D$ has the symmetry $[CK, i\gamma D] = 0$, but now $(CK)^2 = -1$, which allows us to rearrange the matrix elements of the Dirac operator into real quaternions. The corresponding random matrix ensemble is the chGSE.

The ensemble of matrices (10) weighted according to (9) is also known as the Laguerre ensemble. Note that its spectral correlations in the bulk of the spectrum are given by the invariant random matrix ensemble with the same value of β [22].

5. UNIVERSAL PROPERTIES OF THE DIRAC OPERATOR

5.1. Spectral correlations of the lattice QCD Dirac operator

Recently, Kalkreuter [23] calculated *all* eigenvalues of the lattice Dirac operator both for Kogut-Susskind (KS) fermions and Wilson fermions for lattices as large as 12^4 . The ac-

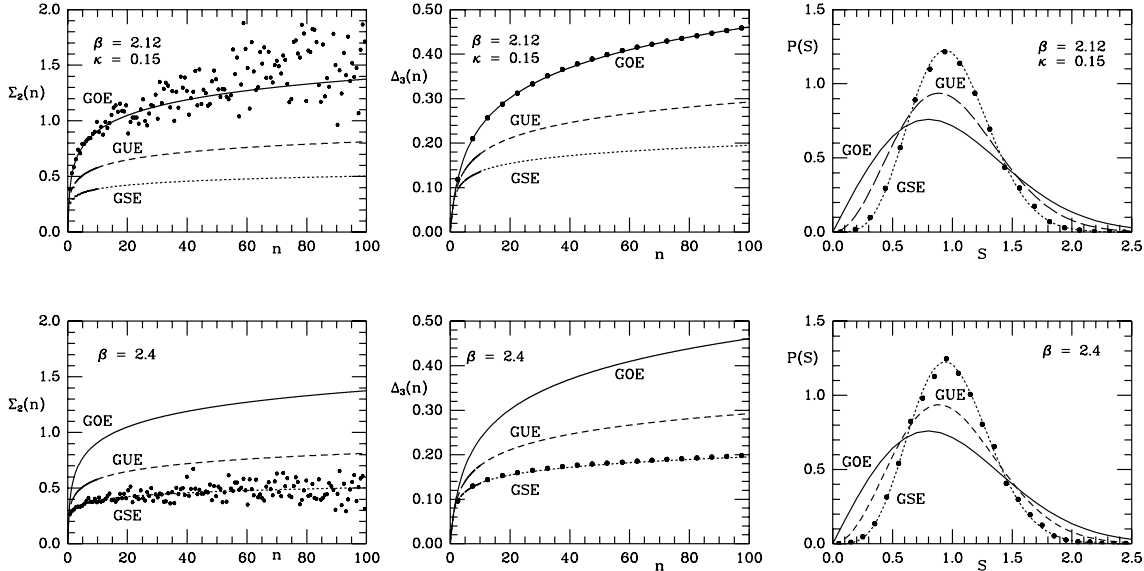


Figure 1. Spectral correlations of Dirac eigenvalues for Wilson fermions (upper) and KS-fermions (lower).

curacy of the eigenvalues was checked via sum rules for the sum of the squares of the eigenvalues the lattice QCD Dirac operator. The anti-unitary symmetry of the KS and Wilson Dirac operator is different. For KS fermions we have [24], $[\tau_2 K, D^{KS}] = 0$, with $(\tau_2 K)^2 = -1$, whereas for the *Hermitean* Wilson Dirac operator, $[\gamma_5 C K \tau_2, \gamma_5 \gamma D^{\text{Wilson}}] = 0$, with $(\gamma_5 C K \tau_2)^2 = 1$. Therefore, we expect that the eigenvalue correlations are described by the GSE and the GOE, respectively [25]. In Fig. 1 we show the result for $P(S)$, $\Sigma_2(n)$ and $\Delta_3(n)$. The results for KS fermions are for 4 dynamical flavors with $ma = 0.05$ on a 12^4 lattice. The results for Wilson fermion were obtained for two dynamical flavors on a $8^3 \times 12$ lattice. The values of β and κ are given in the label of the figure. For a discussion of other statistics we refer to [26].

An interesting question is the fate of spectral correlations for KS fermions in the continuum limit. To answer this question we have analyzed the 100-200 eigenvalues closest to zero. Even for the weakest coupling that was studied ($\beta = 2.8$) no deviation from the GSE was seen.

5.2. Microscopic spectral density for a liquid of instantons.

The investigation of the microscopic spectral density requires a very large number of independent gauge field configurations, which is difficult to generate by a lattice QCD simulations (see however [27]). However, it is possible to simulate a large number of independent instanton liquid configurations. If the microscopic spectral density of such 'smoothed' field configurations is given by chRMM, one certainly expects that this is the case for lattice QCD configurations. In Fig. 2 we show the spectral density of the Dirac operator for $N_c = 2$ and 3, and for 0, 1 and 2 massless flavors [17]. In all cases do we find good agreement with the chRMM prediction. For $N_c = 3$, N_f flavors and topological charge ν it is given by [17]

$$\rho_S(u) = \frac{u}{2} (J_a^2(u) - J_{a+1}(u)J_{a-1}(u)), \quad (11)$$

where $a = N_f + \nu$. The result for $N_c = 2$, which is more complicated, is given in [28]. Qualitatively, the microscopic spectral density has been observed for $SU(2)$ staggered fermions [24] and the lattice Schwinger model [29].

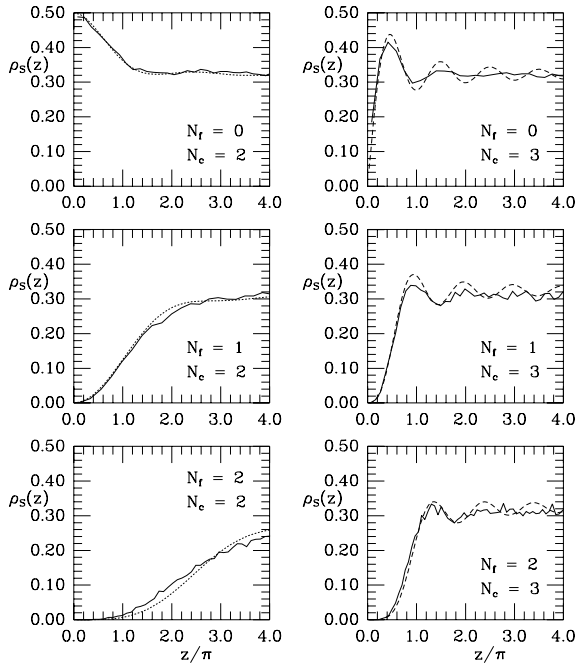


Figure 2. The microscopic spectral density for a liquid of instantons.

5.3. Valence quark mass dependence of the chiral condensate

An alternative way to probe the Dirac spectrum was introduced by the Columbia group [30]. They studied the valence quark mass dependence of the Dirac operator, i.e. $\Sigma(m) = \frac{1}{N} \int d\lambda \rho(\lambda) 2m/(\lambda^2 + m^2)$, for a fixed sea quark mass. In the regime (1), the valence quark mass dependence can be obtained analytically from the microscopic spectral density of (9) [31]

$$\frac{\Sigma(x)}{\Sigma} = x(I_a(x)K_a(x) + I_{a+1}(x)K_{a-1}(x)), \quad (12)$$

where $x = mV\Sigma$ is the rescaled mass and $a = N_f + \nu$. In Fig. 3 we plot this ratio as a function of x for lattice data of two dynamical flavors with mass $ma = 0.01$ and $N_c = 3$ on a $16^3 \times 4$ lattice. We observe that the lattice data for different values of β fall on a single curve. Moreover, in the mesoscopic domain (1) this curve coincides with the random matrix prediction for $N_f = \nu = 0$. Apparently, the zero modes are completely mixed with the much larger number of nonzero modes.

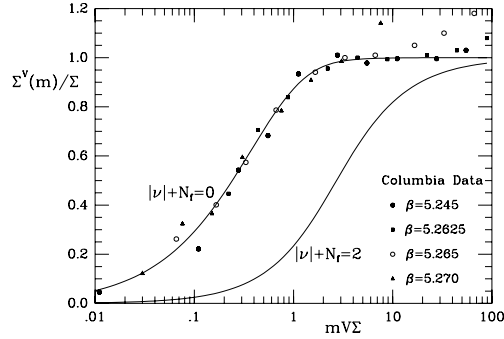


Figure 3. The valence quark mass dependence of the chiral condensate.

For eigenvalues much smaller than the sea quark mass, we expect to see the $N_f = 0$ eigenvalue correlations.

6. SCHEMATIC MODEL THE QCD PARTITION FUNCTION

In this section we review results for a chiral random matrix model with nonzero temperature, T , and chemical potential, μ . The deterministic parts of this model are given by the matrix elements of $\gamma_0 \partial_0 + \mu \gamma_0$ in a basis $\exp[i((2n+1)\pi - \arg P)tT] \phi_n(x)$, where P is the Polyakov loop (introduced in [34]). If the matrix elements of the remaining terms are replaced by the random matrix (10) we arrive at the model [32–36]

$$\mathcal{D} = \begin{pmatrix} 0 & iW + i\Omega_T + \mu \\ iW^\dagger + i\Omega_T + \mu & 0 \end{pmatrix}, \quad (13)$$

where $\Omega_T = T \otimes_n ((2n+1)\pi - \arg P)\mathbf{1}$. Inspired by [37], the simplest model is obtained by keeping only the lowest Matsubara frequency [32,33]. The random matrix model (13) shows a phase transition in T and μ . A related RMT as a schematic model of the Wilson Dirac operator at $T = \mu = 0$ was studied in [38]. Alternative random matrix models for chiral phase transition have been considered as well. I only mention the study of the Dirac operator in the Gross-Witten model, where the transition is driven by the gauge field dynamics [39].

6.1. $T \neq 0$ and $\mu = 0$

The spectral density of the model with only Matsubara frequencies $\pm\pi T$ can be obtained an-

analytically from the solution of a cubic equation [32,34]. It shows a second order phase transition with critical temperature $T_c = 1/\pi\Sigma$ (in the model with one Matsubara frequency) [32]. Such a transition is typical for a 4-fermion model that is obtained after integrating over the random matrices. A particular interesting feature that could be checked by recent lattice studies of the QCD Dirac spectrum [27,40], concerns the fluctuations of the smallest eigenvalue which is qualitatively different below and above T_c [32].

If the phase of the Polyakov line is non-zero, the smallest Matsubara frequency is lower resulting in a higher critical temperature [34]. This result, that can also be obtained from an analysis of the NJL model [41,42], explains recent lattice data by the Columbia group [30] showing that chiral symmetry is restored later for the field configurations with a nonzero Z_3 phase.

Finally, the model (13) provides additional evidence for the universality of the microscopic spectral density [43]. It can be shown that [44], in spite of the dramatic change of the average spectral density, the microscopic spectral density does not change below T_c .

6.2. $\mathbf{T} = \mathbf{0}$ and $\mu \neq 0$

In this section we study the model (13) in the limit $T \rightarrow 0$ at finite N . Note that the $T \rightarrow 0$ limit taken after $N \rightarrow \infty$ is more subtle, *e.g.*, the Fermi-Dirac distribution is obtained only after summing over *all* Matsubara frequencies [45]. For nonzero μ the Dirac operator is no longer Hermitean, and its eigenvalues are scattered in the complex plane. An important question that can be asked in this context is the nature of the quenched limit. In agreement with earlier numerical results by Gocksch [46], Stephanov [35] showed analytically for the model (13) that the quenched limit is obtained as the limit $\lim_{N_f \rightarrow 0} |\det \mathcal{D}|^{N_f}$. The absolute value can be interpreted as the limit of a model with both quarks and conjugate quarks which can produce a Goldstone boson with nonzero baryon number. This explains that $\mu_c \sim \sqrt{m}$ [47] in quenched lattice QCD simulations [35]. For more details, including results for the spectral density, we refer to [48]. A confirmation of some of these results

can be found in [49] The failure of the quenched approximation at $\mu \neq 0$ was also observed for a one-dimensional $U(1)$ model [50].

In the unquenched case, the random matrix model shows a phase transition at $\mu_c = 0.53$ [35,36]. By putting the determinant inside the operator, the resolvent of the Dirac operator, $G(z) = \text{Tr}(z - \mathcal{D})^{-1}$, can be obtained numerically. For z inside the domain of the eigenvalues, it diverges in the thermodynamic limit, and is different from the quenched result obtained analytically in [35]. For z outside this domain quenched and unquenched results coincide in the thermodynamic limit [36]. The same phenomenon is observed [36] for the $U(1)$ model of [50].

7. DISCUSSION AND CONCLUSIONS

We have shown that the spectrum of the QCD Dirac operator shows universal features that can be obtained from a random matrix model with the global symmetries of QCD. In this way, we have obtained analytical results for the finite volume corrections to the valence quark mass dependence of the chiral condensate and the spectral correlations in the bulk of the spectrum. We have also shown that an extension of this random matrix model provides a schematic model for the chiral phase transition. Interesting results have been obtained for QCD at nonzero temperature and at nonzero chemical potential.

This work was partially supported by the US DOE grant DE-FG-88ER40388.

REFERENCES

1. C.E. Porter, '*Statistical theories of spectra: fluctuations*', Academic Press, 1965; R. Haq, A. Pandey and O. Bohigas, Phys. Rev. Lett. **48** (1982) 1086.
2. P. Di Francesco, P. Ginsparg, and J. Zinn-Justin, Phys. Rep. **254** (1995) 1.
3. H.J. Sommers, A. Crisanti, H. Sompolinsky and Y. Stein, Phys. Rev. Lett. **60** (1988) 1895.
4. W. Hauser and H. Feshbach, Phys. Rev. **87** (1952) 366.
5. J.J.M. Verbaarschot, H.A. Weidenmüller and M.R. Zirnbauer, Phys. Rep. **129** (1985) 367.
6. B.L. Altshuler, P.A. Lee and R.A. Webb

- (eds.), *Mesoscopic Phenomena in Solids*, North-Holland, New York, 1991; A. Altland and M.R. Zirnbauer, cond-mat/9602137.
7. P.W. Anderson, Phys. Rev. **109** (1958) 1492.
 8. D.J. Gross and E. Witten, Phys. Rev. **D21** (1980) 446.
 9. H. Leutwyler and A. Smilga, Phys. Rev. **D46** (1992) 5607.
 10. T. Banks and A. Casher, Nucl. Phys. **B169** (1980) 103.
 11. E.V. Shuryak and J.J.M. Verbaarschot, Nucl. Phys. **A560** (1993) 306.
 12. O. Bohigas, M. Giannoni, Lecture notes in Physics **209**, Springer Verlag 1984, p. 1; T. Seligman, J. Verbaarschot, and M. Zirnbauer, Phys. Rev. Lett. **53**, 215 (1984); T. Seligman and J. Verbaarschot, Phys. Lett. **108A** (1985) 183.
 13. F.J. Dyson and M.L. Mehta, J. Math. Phys. **4** (1963) 701.
 14. A.M. Odlyzko, Math. Comp. **48** (1987) 273.
 15. H.D. Gräf *et al.*, Phys. Rev. Lett. **69** (1992) 1296; S. Deus, P.M. Koch and L. Sirko, Phys. Rev. **E53** (1995) 1146.
 16. O. Bohigas, M.J. Giannoni and M.J. Schmit, Phys. Rev. Lett. **52** (1984) 1.
 17. J. Verbaarschot, Phys. Rev. Lett. **72** (1994) 2531; Phys. Lett. **B329** (1994) 351; Nucl. Phys. **B427** (1994) 434.
 18. J.J.M. Verbaarschot and I. Zahed, Phys. Rev. Lett. **70** (1993) 3852.
 19. M. Nowak, J.J.M. Verbaarschot and I. Zahed, Phys. Lett. 217B (1989) 157; Yu. A. Simonov, Phys. Rev. **D43** (1991) 3534.
 20. A. Smilga and J. Verbaarschot, Phys. Rev. **D51** (1995) 829; M.A. Halasz and J.J.M. Verbaarschot, Phys. Rev. **D52** (1995) 2563.
 21. M. Peskin, Nucl. Phys. **B175** (1980) 197; S. Dimopoulos, Nucl. Phys. **B168** (1980) 69; M. Vysotskii, Y. Kogan and M. Shifman, Sov. J. Nucl. Phys. **42** (1985) 318; D.I. Diakonov and V. Yu. Petrov, Lecture notes in physics, **417**, Springer 1993.
 22. H.S. Leff, J. Math. Phys. **5** (1964) 763; D. Fox and P.B. Khan, Phys. Rev. **134** (1964) B1152; B.V. Bronk, J. Math. Phys. **6** (1965) 228; T. Nagao and M. Wadati, J. Phys. Soc. Jap. **60** (1991) 3298, **61** (1992) 78, 1910.
 23. T. Kalkreuter, Comp. Phys. Comm. **95** (1996) 1; Phys. Lett. **B276** (1992) 485; Phys. Rev. **D48** (1993) 1926.
 24. S.J. Hands and M. Teper, Nucl. Phys. **B347** (1990) 819.
 25. M.A. Halasz and J.J.M. Verbaarschot, Phys. Rev. Lett. **74** (1995) 3920.
 26. M.A. Halasz, T. Kalkreuter and J. Verbaarschot, this proceedings.
 27. R. Wensley, this proceedings; J. Stack and R. Wensley, in progress; J. Kogut, J.F. Lagae and D. Sinclair, this proceedings.
 28. J. Verbaarschot, Nucl. Phys. B426 (1994) 559.
 29. H. Dilger, Int. J. Mod. Phys. **C6** (1995) 123.
 30. S. Chandrasekharan, Lattice 1994, 475; S. Chandrasekharan and N. Christ, Lattice 1995, 527; N. Christ, this proceedings.
 31. J.J.M. Verbaarschot, Phys. Lett. **B368** (1996) 137.
 32. A.D. Jackson and J.J.M. Verbaarschot, Phys. Rev. **D53** (1996) 7223.
 33. T. Wettig, A. Schäfer and H.A. Weidenmüller, Phys. Lett. **B367** (1996) 28.
 34. M. Stephanov, Phys. Lett. **B275** (1996) 249.
 35. M. Stephanov, Phys. Rev. Lett. **76** (1996) 4472.
 36. M.A. Halasz, A. Jackson and J. Verbaarschot, in preparation.
 37. A. Kocic and J. Kogut, Nucl. Phys. **B455** (1995) 229.
 38. J. Jurkiewicz, M. Nowak and I. Zahed *et al.*, hep-ph/9603308.
 39. S. Chandrasekharan, MIT-CTP-2530.
 40. K. Jansen and C. Liu, this proceedings.
 41. P.N. Meisinger and M.C. Ogilvie, hep-lat/9512011.
 42. S. Chandrasekharan and S. Huang, Phys. Rev. **D53** (1996) 5100.
 43. E. Brézin, S. Hikami and A. Zee, Nucl. Phys. **B464** (1996) 411. S. Nishigaki, hep-th/9606099.
 44. A.D. Jackson, M.K. Sener and J. Verbaarschot, Nucl. Phys. **B** (1996).
 45. J. Kapusta, *Finite Temperature Field Theory*, Cambridge University Press, 1989.
 46. A. Gocksch, Phys. Rev. Lett. **61** (1988) 2054.
 47. I. Barbour *et al.*, Nucl. Phys. **B275** (1986) 296; M.P. Lombardo, J. Kogut and D. Sin-

- clair, hep-lat/9511026.
48. M. Stephanov, this proceedings.
 49. R. Janik, *et al.*, hep-ph/9606329.
 50. P.E. Gibbs, Phys. Lett. **B182** (1986) 369.